Design, Manufacture, and Validation of a Student-Made Ringsail Parachute for Sounding Rocket Recovery

Thomas Britting[1], Isabelle Joosten[2], Bram Koops[2], Wesley Leonardus Jacobus Rudolf Toussaint[2], Mohamed Sahir Sujahudeen[2], Kristina Vukosavljević[2], Niklas Emil Knöll[2], Adriano Casablanca[2], Nachiket Dighe[2], Sebastian Oliver Scholts[2], Soham Kumar[2], Tom van der Wee[2]

Abstract

In the previous years, the Parachute Research Group (PRG) of Delft Aerospace Rocket Engineering (DARE) has been relying mainly on cruciform, ribbon, or disk-gap-band parachutes for the retrieval of its capsules and smaller sounding rockets. However, heading towards a more sustainable future, with the prospect of full rocket recovery and reusability of larger flagship missions in the future, a new, high-performance main parachute had to be developed. As a result of these, a ringsail-type parachute was selected because of its excellent reefing capabilities, good drag performance, and flight heritage within the professional industry. This paper will focus on three main phases of the development of the new parachute type. Firstly, detailed designs and selection of these different designs created will be presented. Furthermore, considering the fact that this type of parachute is notoriously difficult to produce, new manufacturing methods will be proposed and discussed. Lastly, the results of the wind tunnel tests performed will evaluate and further elaborate on the drag performance, stability characteristics, inflation loads, and reefing capabilities of this parachute type.

Keywords

Ringsail, Sounding rocket recovery, Parachute production

[1]Corresponding author: Delft Aerospace Rocket Engineering, the Netherlands, thomasbritting8@gmail.com.

[2] Delft Aerospace Rocket Engineering, the Netherlands.

Acronyms/Abbreviations

DARE	*Delft Aerospace Rocket Engineering*
PRG	*Parachute Research Group*
OJF	*Open Jet Facility*

1. Introduction

The Parachute Research Group (PRG) of Delft Aerospace Rocket Engineering (DARE) is a sub-team within a student rocket society located in the Netherlands. PRG develops new entry, descent and landing technologies for major flagship missions of DARE, such as the Stratos sounding rockets. DARE has relied mainly on cruciform and disk-gap-band parachutes as low-production-effort and high performance main parachutes respectively [1].

As DARE aims to increase the recovered payload mass to achieve a higher degree of reusability, a parachute with a higher drag coefficient than the current designs is more beneficial. Thus, the development of a parachute type previously unexplored by PRG was selected: the ringsail parachute.

Although large ringsails have been produced in the past for space missions, the characteristics of small scale ringsails are still relatively unknown [2]. The design, manufacturing and wind tunnel testing of four ringsail variants is presented in this paper - alongside the reflections and recommendations.

2. Design selection

Ringsail parachutes are notable for their geometric profile, consisting of annular cloth strips called sails which are spaced apart by slots around the crown, but adjacent towards the skirt. In addition to varying traits such as those offered by most solid parachutes (gore count, vent size, profile angle, etc.), variations may also be distinguished through features intrinsic to the ringsail, like sail fullness (leading and trailing edge widths of each sail), cloth and slot widths, and the angles of attack of each cloth-ring. The aforementioned geometric versatility hence allows for a more adjustable design to attain favourable drag, stability, inflation, and stress relief characteristics. Some ringsails have distinct design features that warrant specific names, these are for example disksails, starsails, and modified ringsails [3]. A disksail is a ringsail that replaces the inner rings around the canopy vent with a circular flat disk. The starsail is a ringsail where multiple gores are replaced by solid gores, which creates a star pattern. The modified ringsail uses wide slots with a conical or biconical profile. Considered separate from ringsail-like designs but within the slotted-parachute category, ringslot parachutes utilise concentric rings instead of individual sails.

The design requirements of a ringsail follow directly from the recovery or overall system requirements. This may include the required descent velocity, deployment conditions, system stability margins, payload weight, as well as internal volume and weight characteristics. These can then be translated into the constructed and geometrical parameters used in the parachute's design and are often based on past ringsail models. However, the scales of historical ringsails used in literature are significantly larger than the target designs in this paper.

Two standard, unmodified ringsails were initially designed by independent sub-groups. For Ringsail A, the team used Section 5: Design Procedures of the "Ringsail Parachute Design" by the Northrop Corporation [4] to calculate and select the necessary parameters to fully design the ringsail. Since the goal was to design a prototype ringsail, the nominal diameter was fixed to 1 m. A smaller diameter would lead to issues with cloth stiffness and a larger diameter would lead to an excessive blockage factor in the wind tunnel. The design guide in the Northrop Corporation book uses empirical relations and data from previous ringsails with nominal diameters between 6 m and 55 m. This means that several empirical relations did not scale well and assumptions had to be made. An example of this is the number of gores, which would be 3 when using the empirical relations, but was nevertheless chosen to be 8 to ensure a round, inflated profile while limiting the production time. Subsequently, the number of sails per gore was computed to be 9, the geometric porosity to be 8.5% and the profile to be 20º conical.

After finishing the first ringsail, the team noticed that a few steps of the manufacturing process could be simplified and therefore decided to create a simple ringslot hybrid parachute. The main differences between ringsails A and B are that the number of sails was reduced and the inner three rings were replaced by ringslots, which lack fullness and could thus be cut as single pieces without connections. Additionally, the sails had a larger relative fullness. As the development of the hybrid parachute progressed faster than expected, a disksail was also conceived and manufactured. This took the form of a modification to ringsail B by means of a disk attached over the vent and inner three rings, which resulted in minimal manufacturing time. The disksail has a lower geometrical porosity in the crown compared to ringsail B, increasing the expected drag.

Ringsail C was designed similarly to ringsail A: using the workflow described by the Northrop Corporation, but with some changes made to its geometry. The geometric porosity was increased to 11.5% by means of a larger vent and wider slots; 7 sails were selected to go with 12 gores to better resemble a hemispherical canopy profile. A slightly lower nominal diameter of 0.9 m and a larger cloth width size of 6 cm were selected to reduce manufacturing overhead. The increase in geometrical porosity close to the crown was chosen to reduce the shock factor associated with parachute inflation. However, it would also go on to aid with reducing the difficulty of attaching an extra ring of sails, with a narrower cloth width than the other sails. The gore templates and side profiles can be seen in Figure 1.

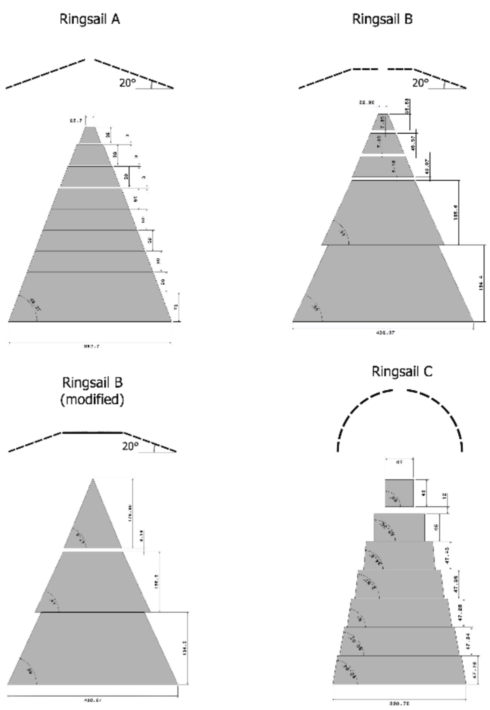

Figure 1: Side profiles and gore templates of the different ringsails.

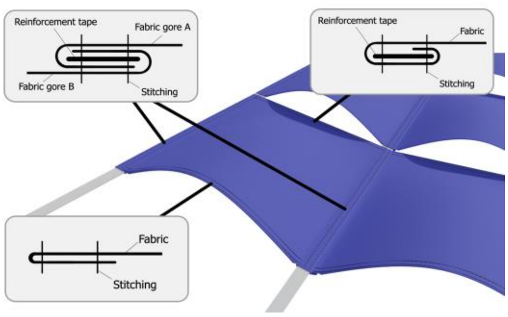

Figure 2: Graphical overview of the different reinforcements on each of the sails.

3. Manufacturing

Once the designs were selected, DXF files of all the sails were needed for use on the laser and fibre cutter. The DXF files, exported from CAD software, were used to cut the sails out of the fabric. This ensured that the dimensions of the sails were accurate and reduced manufacturing time compared to manually cutting the sails. Automating the cutting of fabric eliminated human error. An additional benefit was that the laser slightly melted the edges of the fabric, preventing fraying during the rest of the manufacturing process. Ringsail C was instead cut out on a computer-controlled fibre cutter, which had similar speed and accuracy benefits but did not prevent fraying.

The next step was to reinforce the edges of the sails. As more stress was expected on the trailing edge of the sails (the edge closer to the crown), this side was reinforced with a nylon reinforcement tape. The leading edge was simply folded over itself and stitched down. More reinforcement tape was used to connect neighbouring sails to each other and to function as a load path from the sails down to the suspension lines. These tapes were measured and marked at the correct locations for sail attachments, and then the reinforced sails were attached using the connections shown in Figure 2. The connections were secured using small clothing irons and heat-activated glue before being sewn together, rather than using pins.

Once the canopy was assembled, the lower ends of the vertical reinforcement tapes were folded back and stitched down over themselves to create loops. These loops were connected to the wind tunnel test riser using suspension lines, a link and a swivel.

In the end, each ringsail took between 50 and 100 man-hours to manufacture, except the disksail which was a simple modification of ringsail B. It should be noted that the manufacturing times are not necessarily representative as all ringsails, especially ringsail A, involved some measure of trial and error.

4. Testing

The key objectives of the wind tunnel tests are to quantify the drag, drag coefficient, shock load factor during inflation, and the stability of the ringsail parachutes. For ringsails the shock load factor is typically low, meaning that the inflation forces are not as high. Since this load factor is often the defining load for sizing the suspension lines, riser and structure, decreasing this factor could have a large impact on the design.

Each ringsail was tested under multiple reefing conditions. The reefing percentage is defined as the restricted circumference over the unreefed circumference of the ringsail. All ringsails were reefed to 5%, 10% and 25%.

The tests were conducted in the Open Jet Facility (OJF) of the TU Delft. This wind tunnel has a throat width and height of 2.85 m and can reach speeds up to 35 m/s. The ringsails were attached to a load cell which was mounted to a test bench and can record measurements with frequencies up to 10 kHz, which has proven to be sufficiently fast to capture the inflation shock load for the current set-up. The latter was both bolted to a table in the test chamber and secured with steel cables.

The experiments performed in the OJF were subject to multiple test conditions. The airflow velocity in the wind tunnel was controlled and tests were conducted at speeds up to 27 m/s. The deployment method of the ringsails in the wind tunnel varied for each ringsail variation and test. Deployment could be manual where once the wind tunnel reaches the desired velocity, the ringsail was released into the airflow by hand. In order to test the inflation behaviour, the ringsails could also be deployed from a 3D printed canister using a parachute bag and a pilot chute. These tests could be actuated either by a remotely operated servo or by pulling a string.

All ringsails were tested between 4 and 8 times under reefed and unreefed conditions. During the tests, the ringsails were manually deployed at 10 m/s or out of the canister at 27 m/s. During certain trials, ringsails were deployed at lower speeds and the airflow velocity was progressively increased to test the ringsail at multiple velocities.

5. Results

For each ringsail, the drag coefficient is averaged over the different data points and different velocities at which the ringsails were tested. These average C_d values are presented in Table 2, along with the opening shock load factor of each parachute. This non-dimensional value represents the maximum peak load experienced at inflation, divided by the average steady state load at the deployment velocity. All deployment tests were performed by using a parachute bag and extraction by a pilot chute. Finally, the drag coefficient of the reefed ringsails is presented, expressed as a percentage of the average steady state drag coefficient of the non-reefed ringsails. The stability of each ringsail was tested qualitatively in a wind tunnel, results were recorded in the form of video footage and written observations. Initially, ringsails A and B appeared quite unstable, showing significant lateral movement. It was discovered that manufacturing defects and inconsistent suspension line length were probable causes for this instability. These defects were corrected by the team in between tests, and afterwards each ringsail showed a significant increase in lateral stability. Rotationally, the ringsails showed varying degrees of movement, with ringsail A rotating the most and ringsail B rotating the least. This can likely be explained by the fact that ringsail B is made up of fewer sails, thus containing fewer connections between sails meaning there is a smaller chance for manufacturing errors to occur. However, ringsail B did show more lateral movement than ringsails A and C after being corrected. It should be noted that both the lateral and rotational stability of the ringsails improved when the parachutes were tested in reefed configuration.

With the dynamic pressure and drag known for each wind tunnel test, the drag coefficient was calculated. The choice for reference area to calculate the drag coefficient is arbitrary, as long as the values are consistent with each other. In Table 2, the drag coefficient using the production area and projected area are used. The former area is that of the actual parachute fabric of the ringsail, while the latter area is that of a flat circle with the nominal diameter (mentioned in Table 1). The drag coefficient, using the production area, is very similar for all ringsails, in the order of 0.62 to 0.65, with the disksail (ringsail B modified) exhibiting the lowest performance by a small margin. According to literature [3], the drag coefficients of standard ringsails (such as ringsail A, C) is in range 0.75-1.00 whereas that of modified ringsails (namely ringsail B) is of order 0.65-0.70 [4]. The production and projected area of the ringsails are similar to each other, except for ringsail C due to the hemispherical profile. This also means that there is not a very large difference between drag coefficients using these two different areas for ringsails A, B and modified B, as can be seen in Table 2.

The opening load factor is an important parameter to consider when performing parachute trade-offs or when designing recovery systems, as the inflation shock is typically the highest load the system has to sustain. Ringsail A showed an exceptionally good inflation behaviour with no distinct peak value. Ringsail B and its modified variant had a significantly larger shock load of 1.74 and 1.86 respectively. This discrepancy in shock loading is likely caused by the lower geometric porosity and larger sails of ringsail B, compared to A. During the deployment tests of ringsail C, the pilot chute that extracts the parachute bag was entangled with the pull line. After several seconds, the pilot chute still managed to pull away the bag. No distinct inflation shock load was observed, however the data of this test is marked non-representative. Edgars et al. [4] states that the maximum opening load factor (for a cluster of 2 ringsails) is of order 1.5, for similar dynamic pressures.

The selected reefing ratios gave significant reductions in drag, however the reduction in drag was inconsistent between the different parachutes. Ringsails A and C, both with a relatively high number of sails, had similar amounts of drag reduction. For the two larger reefing line ratios this lines up with literature for ringsails, while for smaller reefing line ratios stiffness likely plays a role in small parachutes [5]. For ringsail B and its modification the drag reduction is significantly smaller. Here the drag reduces significantly between the larger two reefing line ratios, while reefed to 5% the drag does not reduce much further. The reefing behaviour is also largely not influenced by the disksail modification. For the 5% reefing line ratio for ringsail C it was observed that larger velocities were needed for complete inflation of the parachute. During the reefed operation of the different ringsails, flutter on the leading edge sails was observed. This was especially violent for the disksail variant, leading to two of the loops of reinforcement tape connecting to the suspension line failing.

The reductions in drag correspond well to the values for large ringsails according to literature with small deviations [5]. These are to be expected as literature also mentions fabric stiffness as a larger problem for reefing of smaller parachutes.

6. Conclusion

The design, manufacturing, and testing of four ringsails have been presented. The existing design guidelines for ringsails had to be adapted to smaller sizes, by defining a fixed nominal diameter and number of gores, and subsequently computing the geometry based on empirical data. This resulted in four parachutes being manufactured and tested successfully during a wind tunnel campaign. Ringsail A was developed as a prototype, with the goal of further understanding the empirical design relations required to manufacture a small ringsail. Ringsail B was designed to examine the characteristics of a ringsail/ringslot hybrid which was later modified to obtain a disksail. Ringsail C was distinct from the other ringsails by number of gores, crown porosity, and hemispherical profile. Manufacturing was carried out using new methods by cutting the fabric with a laser cutter or fibre cutter. Testing was done in a wind tunnel with speeds up to 27 m/s and varying deployment methods. The results showed that the parachutes were relatively unstable but that reefing improved stability. Furthermore, the drag coefficient for the parachutes was in the order of 0.62 to 0.65. Ringsail A displayed good inflation behaviour with no distinct peak shock load, while for ringsail B and ringsail B modified the inflation load factor was 1.74 and 1.86 respectively. Due to problems with the deployment method of parachute C, no reliable data was collected. Finally, a positive relationship was determined between the reefing ratio and a decrease in drag coefficient.

7. Reflection and recommendations

During the first wind tunnel tests, the team discovered that manufacturing errors were the probable cause for parachute instability. The two most significant deviations were the lengths of the suspension lines and the size of one particular sail. After these were corrected, the stability was noticeably improved. Small manufacturing defects have a large effect on the performance for small parachutes. Therefore, it is highly recommended to perform a more thorough quality control on smaller parachutes.

After consulting the design guides available in literature, it was found that the sails on the relatively small ringsail parachutes described in this paper had a large aspect ratio. During wind tunnel testing it was found that these experience a high-frequency flutter at the canopy's leading edge, both in a reefed and non-reefed configuration. It is recommended to either increase the number of gores or to reduce the number of sails per gore to decrease the sail aspect ratio. The former will however increase the production time significantly.

During the experiment possible sources of error occurred that made the data less representative compared to flight conditions. Two of these were the blockage factor of the parachute and turbulence caused by the test bench, which led to a lower measured drag force.

After wind tunnel testing, it is recommended to flight test a parachute under more representative conditions compared to the controlled environment in a wind tunnel. A test flight of ringsail C on board of PRG's Parachute

Investigation Project rocket is scheduled to launch in March 2022 [6].

Although the stability of the ringsails at reefed conditions was determined during the latest wind tunnel campaign, deployment tests at reefed conditions were not performed. However, it is recommended to characterise the opening load factors of a reefed ringsail in future testing.

Additionally, it is recommended to investigate whether different folding methods can decrease the inflation shock loads of the ringsails. Additional tests may be performed to investigate the effect of geometric porosity on the inflation behaviour.

Acknowledgements

The authors would like to thank the Faculty of Aerospace Engineering at the Delft University of Technology and its staff for their continued support in recovery system testing and the provision of the OJF wind tunnel.

References

[1] L. Pepermans et al, Evolution and Evaluation of the DARE Large Envelope Advanced Parachute System, *FAR Conference*, Monopoli, Italy, 2019.

[2] P. Delurgio, Evolution of the Ringsail parachute, *15th Aerodynamic Decelerator Systems Technology Conference*, AIAA 1999-1700, 1999.

[3] K. Gonyea et al, Aerodynamic Stability and Performance of Next-Generation Parachutes for Mars Entry, Descent, and Landing, *AIAA Aerodynamic Decelerator Systems Conference,* AIAA 2013-1356, 2013.

[4] E.G. Ewing, Ringsail Parachute Design, Northrop Corporation, 1972.

[5] T.W. Knacke, Parachute Recovery Systems Design Manual, Para Publishing, 1991.

[6] M. Géczi, L. Pepermans, G. Kandiyoor, O. Dvořak, Development of a low cost, low altitude test vehicle for high dynamic pressure parachute testing, *International Astronautical Conference*, the CyberSpace Edition, 2020.

Table 1: Overview of the different ringsail designs.

Parameter	Ringsail A	Ringsail B	Ringsail B (modified)	Ringsail C
Type	Ringsail	Modified ringsail	Disksail	Ringsail
Gores	8	8	8	12
Gore composition	9 sails	2 sails, 3 slots	2 sails, 1 disk	7 sails
Nominal diameter [m]	1.0	1.0	1.0	0.9
Production area [m^2]	0.792	0.888	0.904	0.550
Projected area [m^2]	0.785	0.785	0.785	0.414
Profile	20° conical	Biconical (20°-0°)	Biconical (20°-0°)	Hemisphere
Suspension line length [m]	1.15	1.15	1.15	1.08
Material [-]	F-111	Kite fabric	Kite fabric	Kite fabric

Table 2: Overview of drag performance of the different ringsails under different conditions.

Parameter	Ringsail A	Ringsail B	Ringsail B (modified)	Ringsail C
Type	Ringsail	Modified ringsail	Disksail	Ringsail
C_d average w.r.t. production area [-]	0.64	0.64	0.62	0.65
C_d average w.r.t. projected area [-]	0.65	0.72	0.72	0.87
Opening load factor, deployed from parachute bag [-]	1.00	1.74	1.86	Unreliable data
Percentage of C_d, reefed to 25%	39.5%	55.2%	61.2%	37.5%
Percentage of C_d, reefed to 10%	15.8%	36.9%	34.9%	14.0%
Percentage of C_d, reefed to 5%	8.9%	31.0%	-	5.8%